# OPTIMIZATION OF THE GEOMETRY OF A HEAT SINK

Matthew B. de Stadler
Advisor: Hossein Haj-Hariri
*University of Virginia, Charlottesville, VA 22904*

## Abstract

Cellular materials have properties similar to conventional materials on the macroscopic level but possess several advantages at the microscopic level, including the ability to be manufactured down to a very small scale. With this ability, new geometric configurations for a heat sink are able to be considered. This paper details the results of a study to develop a geometry based optimization tool for heat sink design. With the principle of superposition, the analysis of a heat sink can be simplified by using a repeating cell. For the repeating cell, the following questions are posed: Given a certain percentage of the volume available for channels for fluid to pass through, where should one place the channels? What shape should they be? To answer these questions a theoretical approach was used with testing and analysis performed using computational fluid dynamics software. Three unsuccessful schemes are presented, with explanations as to why they did not prove successful. Lessons learned from these attempts are applied to the ongoing development of an optimal heat sink for use in skin cooling of a hypersonic vehicle.

## Nomenclature

| | | |
|---|---|---|
| $A$ | = | area |
| $c_p$ | = | specific heat capacity |
| $h$ | = | convection heat transfer coefficient |
| $H$ | = | height |
| $k$ | = | thermal conductivity |
| $L$ | = | length |
| $\dot{m}$ | = | mass flow rate |
| $n$ | = | number of channels |
| $\rho$ | = | density |
| $p$ | = | pressure |
| $P$ | = | power |
| $Q$ | = | heat flux |
| $\dot{Q}$ | = | heat flux rate |
| $s$ | = | perimeter |
| $\mu$ | = | dynamic viscosity |
| $T$ | = | temperature |
| $V$ | = | velocity |
| $W$ | = | width |

## I.  Introduction

Heat sink research and development has had a long history which is still ongoing with efforts to improve design and performance. As Incropera and DeWitt state, "With heightened concern for energy conservation, there has been a steady and substantial increase in activity. A focal point of this work has been *heat transfer enhancement*, which includes the search for special heat exchanger surfaces[*] through which enhancement may be achieved."[1] Recent developments in cellular materials allow for the consideration of designs previously not possible. Cellular materials allow for the construction of very small heat sinks with passageways for fluid to pass through on the order of several millimeters thick as shown in Fig. 1.[2]
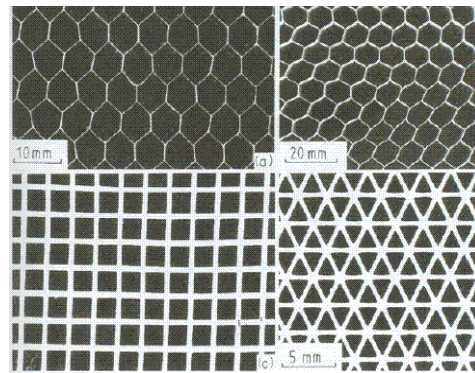


**Figure 1. Cellular structures.[2]**

Their superior properties, when compared with conventional materials, make cellular materials very desirable for a wide range of applications where size, weight, and efficiency are important.

The decision to investigate optimal geometries for heat sinks was inspired by these recent developments. Optimal geometries have enhanced heat transfer surfaces which allows devices to take advantage of one of the following options: size reduction, increased thermodynamic process efficiency which leads to lower operating costs, increased heat exchange rate for fixed fluid inlet temperatures, or reduced pumping power for fixed heat duty.[3]

To the best of the author's knowledge, a study of optimal geometries for a fixed volume rectangular heat sink with a fixed percentage of the volume available for internal channels for cooling fluid has not been conducted. The goal for this paper was to develop a methodology which would allow one to develop an optimal heat sink based on geometrical considerations independent of working fluid choice and heat sink material choice. A general solution was sought so that the results obtained could be use for heat sink

---

[*] also heat sink surfaces.

applications ranging from small-scale electronics cooling to temperature regulation in large energy facilities.

As heat sinks tend to be very complex, the analysis was simplified by considering designs employing a repeating cell. Using the principle of superposition, the characteristics of the entire heat sink may be determined from the characteristics of a representative cell. For a fixed volume cell with a given percentage of the volume available for cooling channels, two questions were posed:

    i.    How should one layout the channels?
    ii.    What shape should the channels be?

A purely theoretical approach was employed to answer these questions, with testing and analysis performed using computational fluid dynamics (CFD) software. Several attempts were made to develop a metric for comparing designs with different features to objectively determine the best one. Each attempt is presented with explanation as to why it was not successful. Current work being done on skin cooling for a hypersonic vehicle is also presented.

The structure of this paper is as follows. Section II presents the problem statement. 2-D conduction modeling efforts are given in Chapter III. Chapter IV details an attempt to generate performance trends. Attempts to develop a performance metric are given in Chapter VI. Skin cooling of a hypersonic vehicle, an application of this general research, is discussed in Chapter VII. Conclusions and future work to be done are presented in Chapter VIII.

## II.   Problem Formulation

To determine an optimal design for a heat sink, the principle of superposition was used to reduce the design area to the smallest repeating cell as shown in Fig. 2.
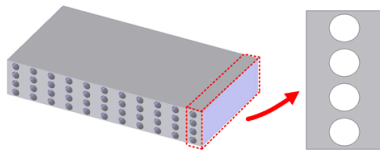


Figure 2. Repeating cell concept.

This allows one to determine the characteristics of the complex heat sink from a simple repeating cell. A fixed percentage of the cell volume is available for channels for fluid to pass through. Within the cell, a number of design variables are able to be considered including:

    (i)    Number of channels
    (ii)    Placement of channels within the normal face of the metallic block
    (iii)   Channel geometry (circle, square, triangle,…)
    (iv)   Channel shape (straight versus coiled tube)
    (v)    Fluid mass flow rate

In addition to passive enhancement techniques like those mentioned above, active enhancement techniques requiring external power such as acoustic fields and surface vibration can be used to improve heat transfer.[3] Attention will be focused on passive techniques due to the limited scope of this paper.

What does it mean for a design to be optimal? For the purpose of this study, an optimal design is one in which the greatest thermal protection is offered at the lowest pumping power. This thermal protection can be quantified using values like the maximum temperature, average temperature, or maximum heat flux. The optimal solution is believed to lie between two extreme cases, one large channel which doesn't remove very much heat but has a very low pumping power and infinitely many small channels which remove a very large amount of heat yet require extremely high pumping power. Another goal of this study was to ensure that the minimum amount of working fluid would be needed to provide the desired cooling.

The situation under consideration is that a device is subjected to a thermally demanding environment and a limited space for cooling is available. A heat sink consisting of a rectangular block with channels for cooling fluid to flow through is placed in between the device and the hot source to offer thermal protection for the device. For this analysis the problem was modeled as shown in Fig. 3(a).
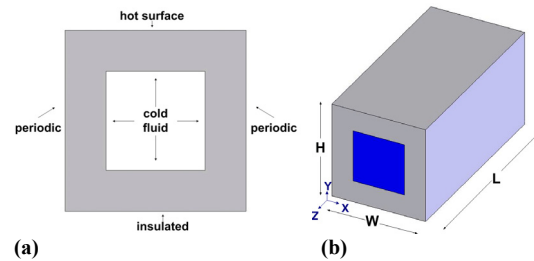


(a)                        (b)
Figure 3. (a) Problem setup. (b) Model dimensions.

The top of the representative unit cell is exposed to a hot surface, a periodic boundary condition is applied to the sides due to symmetry, the bottom is assumed to be insulated, and cold fluid passes through the channels.

Two modes of heat transfer occur in this heat sink: conduction and convection. Figure 4 shows conduction in the metal on the normal face of three different possible designs. Heat is uniformly applied to the top



Figure 4. Temperature profile on the normal face for several geometries. Red is hot and blue is cold.

surface and travels down toward the bottom. All of the

heat is transferred from the block metal to the working fluid by convection but depending on where the heat enters the cooling channel, the average temperature of the metal block will vary. Figure 5 shows the temperature variation in the axial direction for three different mass flow rates through a square duct.
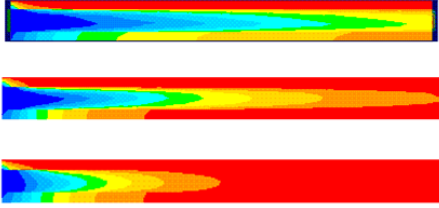


**Figure 5. Temperature profile in the axial direction for flow in a square duct. Red is hot and blue is cold.**

The top design's mass flow rate is too high and results in the fluid exiting the heat sink before it is fully heated. This is undesirable because excessive pumping power is required and the fluid is still able to remove additional heat when it exits the channel. The bottom design's mass flow rate is too small and as a result the fluid becomes fully heated well before it leaves the heat sink. This is undesirable because the fluid stops doing effective thermal work before it leaves the channel. The middle design is very close to the optimal design in that the fluid leaves the heat sink just as it becomes fully hot.

In addition to searching for optimal shapes and layouts for channels, knowledge of the variables governing the ideal mass flow rate is also desired. By applying the conservation of energy to a differential control volume for internal flow in a tube, one can obtain an expression for the mean temperature of the fluid.[1] For flows with a constant surface heat flux the following relationship is obtained:

$$T_m(x) = T_i + \frac{\dot{Q}_s s}{A_s \dot{m} c_p} x \tag{1}$$

Where $T_m(x)$ is the mean fluid temperature as a function of axial position, $T_i$ is the fluid entrance temperature, $\dot{Q}_s$ is the surface heat flux, $c_p$ is the specific heat capacity, s is the channel perimeter, $\dot{m}$ is the mass flow rate and $A_s$ is the exposed surface area. If instead of a constant surface heat flux, a constant surface temperature is used, one finds that.

$$T_m(x) = T_s - (T_s - T_i)e^{\left(-\frac{s h_{avg}}{\dot{m} c_p}\right)x} \tag{2}$$

Where $T_s$ is the hot surface temperature, and $h_{avg}$ is the average heat transfer coefficient at the fluid-metal interface. From Eq. (2) above, one can observe that the ideal channel cooling length, $L_{ch}$, is proportional to the

fluid entrance temperature, hot surface temperature, and the following parameters:

$$L_{ch} \propto \frac{c_p \dot{m}}{s h_{avg}} \tag{3}$$

$$\dot{m} \propto \frac{c_p L_{ch}}{s h_{avg}} \tag{4}$$

Where $\propto$ indicates proportionality. Once the parameters affecting the equilibrium length are determined, the relationship can be re-written for the mass flow rate by fixing the cooling channel length. A similar approach can be used for the constant surface heat flux case. It is important to note that the variables in Eqns. (3) and (4) are not independent and determining an exact solution is not possible for the relations provided in Eq. (2).

The pumping power considerations of this study depend only on the geometry of the channels; they are considered independent of the fluid temperature. For a given flow area, a different pumping power will be required if the channel cross section is a circle, square, or triangle. The channel's location in the block does not make a large difference. The flow is assumed to be incompressible, uniform, fully developed, and fully turbulent. Operating conditions are assumed so that the working fluid does not undergo a phase change.

### III.  2-D Conduction

#### A.  Problem Statement

2-D conduction in a square with a cooling channel was examined to get an idea of the role that conduction would play in this problem. For this scenario, the problem was formulated with the boundary conditions shown in Fig. 6(a).
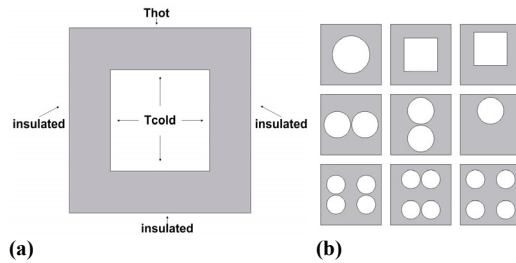


**(a)**                **(b)**
**Figure 6. (a) Boundary conditions. (b) Shapes used for testing.**

The top surface was held at a fixed hot temperature, the sides were modeled as adiabatic due to symmetry, and the fluid-metal interface was modeled as a fixed cold temperature. No heat was transferred from the normal face of the metal block to the surroundings. Several different models were used to obtain insight into how channel shape and placement affect the heat transfer in the cell. The models used for this testing are shown in Fig. 6(b). Each one has thirty percent of the volume

available for channels for fluid to pass through with the exception of the one high circle. That case was chosen to determine how the heat sink would perform without the bottom circle.

## B.  Analysis

All the heat that enters the cell from the top is removed by the working fluid. Therefore, by assuming $\Delta T$ equal to a change of one degree and that that $Q_s = \dot{Q}_s$, the mass flow rate necessary to remove the heat was determined using the relationship:

$$\dot{m} = \frac{\dot{Q}_s}{c_p \Delta T} \tag{5}$$

Where, $\Delta T$ is the change in temperature. From this necessary mass flow rate, as well as the flow area, the necessary pumping power was determined by dimensional analysis.

$$P = p A_{flow} V = \frac{\dot{m}^3}{(\rho A_{flow})^2} \tag{6}$$

Here P is pumping power, V is velocity, p is the pressure, $A_{flow}$ is the flow area, and $\rho$ is the density of the fluid. To compare the different designs, the ratio of heat removed to pumping power was used.

## C.  Results

Using the boundary conditions given in Fig. 6(a) with air as a working fluid, steel as the block material, a hot temperature of $100^{\circ}C$ and a cold temperature of $25^{\circ}C$, computational fluid dynamics (CFD) software was used to run analyses on the models shown above in Fig. 6(b). After each simulation, the heat flux at the top surface was obtained from the CFD program. The pumping power was determined from Eq. (6) above. The results are given below in Table 1.

**Table 1. 2-D Conduction Results**

|  | $\dot{Q}_s$ (W) | $\dot{Q}_s/P$ (dimensionless) |
|---|---|---|
| 1 circle | 147.89 | 0.58 |
| 1 square middle | 155.32 | 0.61 |
| 1 square high | 252.2 | **0.99** |
| 2 circle horizontal | 127.07 | 0.06 |
| 2 circle vertical | 309.75 | 0.15 |
| 1 circle vertical | 309.45 | n/a |
| 4 circle horizontal | 283.67 | 0.02 |
| 4 circle vertical | 179.84 | 0.02 |
| 4 circle equal | 295.15 | 0.02 |

## D.  Discussion of Results

As one can observe from Table 1, designs with one channel greatly outperformed their competitors. This is to be expected from the rough pumping power estimate produced by Eq. (6). A channel size reduction of one half results in a pumping power value four times greater than the original. This result overpowers the increased heat removal rate that is obtained from designs with additional channels.

One does observe however that the designs with channels closer to the hot surface remove significantly more heat than those further away. This occurs because the driving force behind the heat flux is the temperature gradient as illustrated below in Eq. (7).

$$\dot{Q} = k A_n \frac{dT}{dy} \tag{7}$$

Where k is the thermal conductivity, T is the temperature, and $A_n$ is the area normal to the heat flow. Since k and $A_n$ will be the same for each of the trials and the temperature difference between the hot surface and the cold surface will be the same as well, the only variable left to impact the heat flux rate is the vertical distance between the two surfaces. Therefore designs with a smaller distance between the hot surface and flow channels will remove more heat than those located further away. From the one circle vertical case one can observe that essentially all of the heat is removed by the top hole, the lower one in the two circle vertical case offers a negligible benefit.

## IV.  3-D Performance Trends

## A.  Rationale

From the results of the 2-D conduction tests, it was determined that 3-D effects due to length must be considered. By considering the effects of fluid motion, the problem became one of conduction in a solid with forced convection through internal channels as opposed to pure conduction through a solid block. This work was done to gain insight into the relationship between input parameters such as the mass flow rate and channel layout, and output parameters such as the temperature at critical locations and pumping power required. To generate the performance curves, simulations were run for several different values of the mass flow rate with both water and air as a working fluid.

## B.  Problem Statement

For this simulation, the two models shown in Fig. 7(b) were used to generate performance curves.
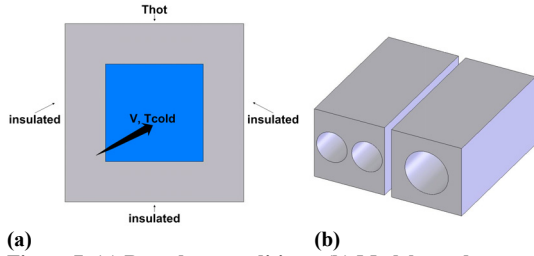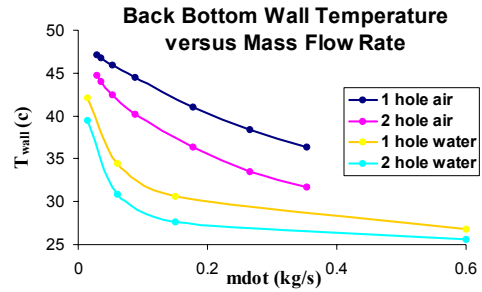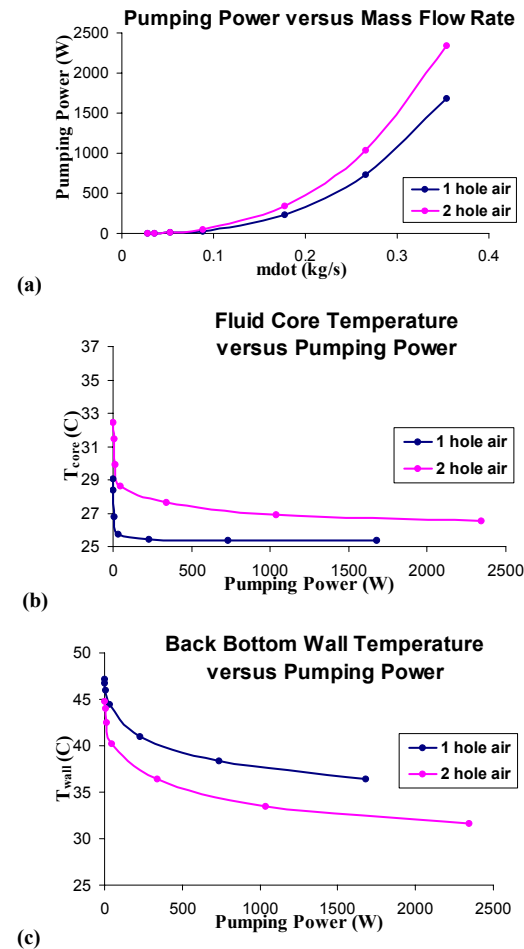
**(a)**            **(b)**

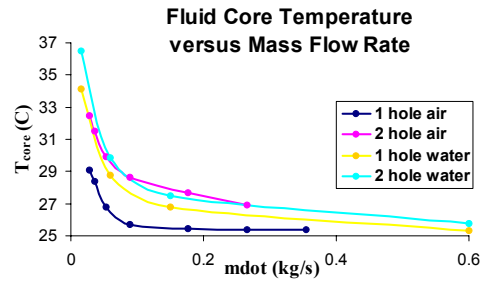**Figure 7. (a) Boundary conditions. (b) Models used.**

As in the 2-D conduction trials, thirty percent of the block by volume was available for fluid to pass through. The boundary conditions shown in Fig. 7(a) were used. These are essentially the same as the conditions used for the 2-D conduction trials with the exception of the fluid now having an inlet temperature and mass flow rate rather than a fixed temperature at the fluid-metal interface. 50°C was used for the hot temperature, the cold fluid temperature was maintained as 25°C, and the block material was kept as steel.

## C. Performance Curves

Figure 8 shows the different performance curves that were generated by these simulations.



**(a)**



**(b)**



**(c)**



**(d)**



**(e)**

**Figure 8. Performance curves.**

## D. Discussion of Curves

From the performance curves above one can observe several trends. Figure 8(a) shows that the pumping power rises in an exponential fashion with mass flow rate. As pumping power increases, the back bottom wall temperature and the fluid core temperature are reduced; this can be seen in Fig. 8(b) and Fig. 8(c). A lower core temperature indicates that the fluid is leaving the channel before becoming fully hot and is therefore not being used as efficiently as possible. The relationship between the mass flow rate and the back bottom wall temperature and the fluid core temperature follows the same trends as the relationship with the pumping power. All the curves show monotonically increasing or decreasing values which will eventually approach an asymptotic value and therefore further work with other shapes was not performed. From the initial trends shown, one can observe that the pumping power for a given mass flow rate increases with the number of channels. Another trend present is that the core fluid temperature increases with the number of channels. Lower back bottom wall temperatures are obtained with greater numbers of channels.

Another option associated with performance curves is to conduct a transient analysis to look at designs which keep the back bottom wall temperature below a critical value for a given time. The initial back bottom wall temperature will be a function of the geometry of the channel, the mass flow rate, the flow area, the hot surface temperature, and the cold fluid temperature. As steady state conditions are approached, the back bottom wall temperature will approach the hot temperature for intensive thermal loads. The back bottom wall temperature versus time curves will be different for

each condition and one could generate data for this situation to determine which design has the lowest temperature at a characteristic time. This analysis is suited for devices which undergo an intense but short duration thermal load.

Water has a much higher specific heat capacity than air and therefore removes a much larger amount of heat for a given mass flow rate. Additional difficulty with using air for these simulations occurs because the incompressibility assumption can easily be violated by flows in the desired cooling flow rate regime. As a result of this testing, water was chosen as the working fluid for further testing and air was abandoned.

One should note that these trials were not very thermally demanding. Each of the designs easily prevented excessive temperatures from being reached. However, these trials were still valuable in that they displayed trends which allowed insight to be obtained.

## V. Performance Metric

### A. Rationale

For optimization purposes, it is useful to have a single quantitative performance measure which can be minimized or maximized as an objective function subject to specific performance constraints.[4] With such a tool, which will henceforth be referred to as a performance metric, it is relatively easy to determine the merits of different designs. This allows one to compare more traditional designs with constant cross-section square ducts to recent designs employing helical tubes like the ones seen in Fig. 9. Recent work studying fluid flow in helical tubes indicates that the higher heat transfer rate obtained from increased fluid mixing outweighs the increased pumping power penalty.[5] Within these helical tubes several



**Figure 9. Helical tube with square cross section.[6]**

variables are able to be considered such as number of coils, number of axes coiled around, twist angle, and the coil radius. Investigating the viability of using coiled tubes in heat sinks is of great interest for further research.
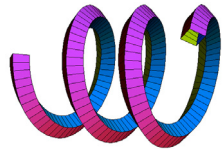
An important tool for efficiently carrying out simulations is the Taguchi method. This statistical technique has shown promise when applied to a CFD study to extend results from incompressible wind tunnel data at moderate Reynolds numbers to flight Reynolds number values,[7] and preliminary results leads the author to believe this tool will greatly reduce the number of simulations required to identify key relationships for this study. In addition, the Taguchi method is useful for determining the importance of the interaction between

different variables which facilitates the development of the desired performance metric.

### B. Problem Formulation

The boundary conditions used in Section IV were kept for this analysis; they can be seen in Fig. 7(a). The different models used for these simulations can be seen in Fig. 10; note that they are 3-D but are shown in 2-D for ease of viewing.
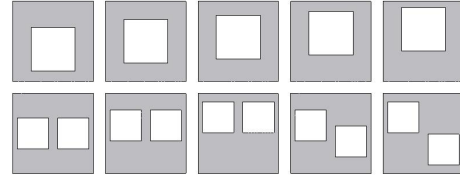


**Figure 10. Geometries used for initial performance metric. The top row of designs are numbered 1,2,3,4,5 and the bottom row are numbered 6,7,8,9,10 respectively for analysis purposes.**

Water was used as the working fluid and steel was used as the block metal.

### C. Analysis

After observing that simply considering the metric of heat removed per unit pumping power did not prove adequate for optimization purposes, greater complexity was introduced in the performance metric. The following four goals were sought for an optimal heat sink:

i. Removes the greatest amount of heat
ii. The fluid just reaches a fully hot state as it exits
iii. The bottom wall temperature is as close to as possible while still below a critical temperature
iv. Uses the smallest amount of pumping power

Each of the above goals was written in the form of an equation and then non-dimensionalized by a problem relevant quantity. The beneficial aspects (goals i,ii,iii) were emphasized while the disadvantageous one (goal iv) was penalized. The following metric was obtained

$$score = \frac{[\dot{Q}/\dot{Q}_0][T_{core}/T_{hot}][T_{bottom}/T_{critical}]}{[P/P_0]} \quad (8)$$

$$\dot{Q}_0 = \frac{k(T_{hot} - T_{in})LW}{H} \quad (9)$$

$$P_0 = \frac{\mu(\dot{m}/\rho A_{hole})^2 LA_{hole}}{H^2} \quad (10)$$

Where k represents the thermal conductivity of the metal, $\mu$ the dynamic viscosity of the fluid, L, W, and H are block dimensions. $Q_0$ was obtained by considering conduction through the block as a plane wall. A differential control volume was used to obtain the pressure difference over the channel length. The

resulting equation for the pressure difference was used in Eq. 6 to find $P_0$, the reference pumping power.

### D. Results

The results from initial testing of the performance metric are given below in Table 2.

**Table 2. Performance Metric Results**

| Design number | $\dot{Q}$ (W) | $T_{core}$ (C) | $T_{bottom}$ (C) | P(W) | Score (normalized) |
|---|---|---|---|---|---|
| 1 | 1261.6 | 25.95 | 32.07 | 1.70E-4 | 0.727 |
| 2 | 1398.0 | 25.95 | 33.44 | 1.66E-4 | 0.824 |
| 3[*] | 1645.2 | 25.98 | 33.32 | 2.23E-4 | 0.725 |
| 4 | 1568.5 | 26.22 | 34.73 | 1.71E-4 | 0.907 |
| 5 | 1695.8 | 26.28 | 35.25 | 1.68E-4 | **1.000** |
| 6 | 1469.5 | 26.83 | 25.59 | 3.34E-4 | 0.427 |
| 7 | 1777.1 | 27.47 | 30.36 | 3.41E-4 | 0.509 |
| 8 | 1980.5 | 27.64 | 30.90 | 3.42E-4 | **0.566** |
| 9[†] | 1594.6 | 27.08 | 30.31 | 3.30E-4 | 0.470 |
| 10[‡] | 1725.2 | 27.73 | 31.11 | 3.67E-4 | 0.461 |

### E. Discussion of Results

The best designs were single channels located as close to the hot surface as possible. The additional pumping power requirements outweighed the increased heat flux benefit from more holes. There was not enough variation in the fluid core and back bottom wall temperatures between the different designs to make much of a difference in the final score.

The fixed temperature boundary condition for the hot surface is not a good choice for the problem. The conduction of the heat through the metal to the top of the cooling channel is driven by the temperature gradient which is maximized by putting the cooling channel as close to the top as possible (cf. Eq. (7) and Table 2). Such implicit dependence of the heat flux on the proximity of the cooling channel to the surface results in the lack of a baseline problem. Without such a baseline case it is not possible to conduct a rational optimization study. A better choice would be to use a constant heat flux boundary condition. A constant heat flux prevents designs with channels located close to the top surface from drawing upon an infinite reservoir of heat.

Designs which have a higher value of heat removed also have a higher back bottom wall temperature. This is due to the fact that more heat is drawn in and not all of it is able to be removed by the top and sides of the cooling channel. Some heat is carried through the channel walls to the bottom section where it builds up

---

[*] These values are believed to be caused by a numerical instability in the CFD program used and should not be considered valid.

[†,‡] The variation in pressure value is indicative of poor CFD results; since the flow geometries are the same there should be less variability

in the area from the insulated bottom surface to the lower channel wall.

Another possible metric would emphasize designs which have the lowest average temperature possible. This would be done by re-writing the performance metric as

$$score = \frac{[\dot{Q}/\dot{Q}_0][T_{core}/T_{avg}]}{[P/P_0]} \qquad (11)$$

An advantage of this formulation is that it now seeks to minimize the average temperature of the heat sink which makes sure the heat sink does not suffer failure due to thermal damage which would lead to failure of the device to be protected. Note that one could also use $T_{max}$ instead of the average temperature.

## VI. Skin Cooling of a Hypersonic Vehicle

### A. Application Background Information

Objects flying at hypersonic speeds experience significant heating due to skin friction drag. Figure 11 shows the heat flux profile on the Hyper-X vehicle at Mach 7. Blue represents low levels of heat flux and red represents regions of high heat flux.
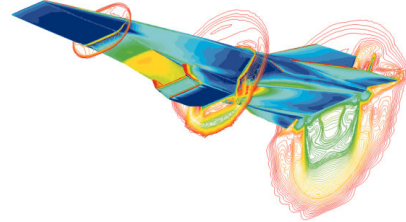


**Figure 11. CFD simulation of the heat flux on the Hyper-X vehicle at Mach 7.[9]**

The leading edges of the vehicle have very high heat flux values, as do locations where the flow turns. This poses a significant challenge for aircraft designers since the temperatures encountered are often above the melting point of materials available. This materials selection problem will only become more difficult as the maximum possible speed continues to increase. It is hoped that cellular materials will be able to be used to construct heat sinks that would be able to provide significant skin cooling as an alternative to current high performance materials. Research has shown that designs with an Aluminum-Niobium alloy and a working fluid with properties similar to water hold promise.[8]

### B. Problem Formulation

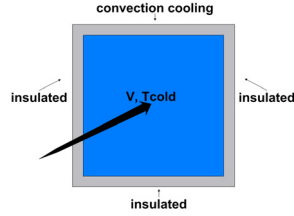A unit cell approach is used with the boundary conditions given in Fig. 12.

**Figure 12. Boundary conditions.**

Unlike the previously used fixed temperature boundary condition for the hot surface, the convection cooling boundary condition is more physically realistic. The shapes considered are limited to squares for this analysis. Symmetry is maintained and designs with $n^2$ channels are considered. This value can be extended from one until a sufficiently large n so that a critically small wall thickness value is reached. Several possible channel layouts are presented in Fig. 13(a) to show the relative wall thickness differences. The length will be much greater than the height for the cooling sections as shown in Fig. 13 (b).
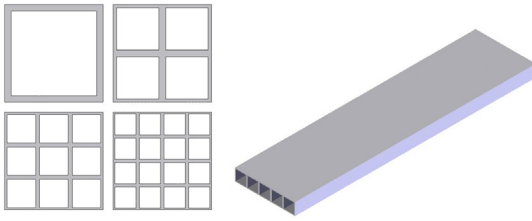

**Figure 13. (a) Possible geometries. (b) Heat sink section.**

In addition to searching for a performance metric, a thermal resistance network approach is being developed. Valdevit et al. used a thermal resistance network analysis with a fin analogy to determine the temperature profile in a square channel and obtained good results.[10] Their approach used separate 1-D analyses in the horizontal and vertical direction which is valid for designs with very thin walls but is less accurate in designs with thicker walls. The network being developed in this paper aims to further generalize the results by being able to obtain reasonable answers for designs where lateral conduction also plays a significant role and 2-D effects need to be considered. It is important to note that the approach being developed could in principle be applied to non-square channels but the analysis would be significantly more difficult.

## C. Thermal Network Setup

Electrical resistance network analogies are a reliable tool for solving heat transfer problems. The information presented below represents initial work on setting up a thermal network to model the heat transfer in thin walled cooling channels. While the material presented is far from complete, key ideas are given that are hoped to lead to improvements over current models

being used, such as the one developed by Valdevit et al.[10]

Table 3 lists the input and output parameters for the thermal network.

**Table 3. Problem Parameters**

| Inputs |
|---|
| Material properties |
| Model dimensions |
| Fluid inlet flow rate |
| Fluid inlet temperature |
| Hot temperature value |
| **Outputs** |
| Node temperatures |
| Node heat fluxes |
| Fluid exit temperature |

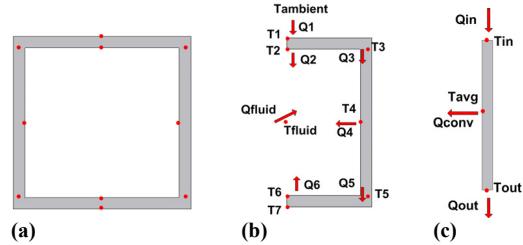Figure 14(a) shows how a thermal network was set up to analyze a square geometry.


**Figure 14. (a) Thermal resistance network nodes.**
**(b) Simplified thermal network with temperatures and heat fluxes shown.**
**(c) Side element illustrated.**

The nodes where heat fluxes and temperature values are calculated are shown as the red dots. By taking advantage of symmetry, the thermal network can be further simplified to the one shown with the relevant temperatures and heat fluxes in Fig. 14(b). Figure 14(c) shows an expanded view of the side element, note that $T_{in}$ corresponds to $T_3$ and $T_{out}$ corresponds to $T_5$. This approach considers the temperature to vary only in the vertical direction; conduction in the horizontal direction is negligible. As these solid walls are very thin, this is not a bad assumption for this case. To find $T_{avg}$, a differential control volume analysis was used to determine the temperature as a function of the y location in the element. From this one is able to calculate the average temperature using the relationship

$$T_{avg} = \frac{1}{H}\int_0^H T(y)dy \qquad (12)$$

Where H is the height of the side piece and T(y) is the temperature profile in the vertical direction.
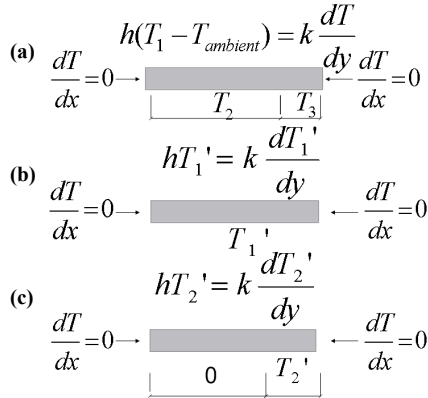
The top piece was modeled as shown in Fig. 15(a).

**(a)**

$$\frac{dT}{dx}=0 \rightarrow \qquad \leftarrow \frac{dT}{dx}=0$$

$$h(T_1 - T_{ambient}) = k\frac{dT}{dy}$$

$$T_2 \quad | \quad T_3$$

**(b)**

$$\frac{dT}{dx}=0 \rightarrow \qquad \leftarrow \frac{dT}{dx}=0$$

$$hT_1' = k\frac{dT_1'}{dy}$$

$$T_1'$$

**(c)**

$$\frac{dT}{dx}=0 \rightarrow \qquad \leftarrow \frac{dT}{dx}=0$$

$$hT_2' = k\frac{dT_2'}{dy}$$

$$0 \qquad T_2'$$

**Figure 15. Heat conduction in the upper right corner.**
**(a) Case 1 boundary conditions.**
**(b) Case 2 boundary conditions.**
**(c) Case 3 boundary conditions.**

Rather than try to solve for the temperature distribution with such difficult boundary conditions, the problem was broken down using the principle of superposition into two simpler problems as shown in Fig. 15(b) and Fig. 15(c). In Fig. 15(b), $T_1'=T_3-T_{ambient}$ and in Fig. 15(c) $T_2'=T_2-T_3$. Note that a Fourier Cosine Series is used to represent the step function on the bottom surface boundary condition in case 3. Once one solves the governing equation for 2-D steady state heat conduction in a solid

$$\nabla^2 T = 0 \qquad (13)$$

for cases 2 and 3 throughout the rectangle to obtain the temperature distribution in the area, one can integrate the heat flux per length at the top and bottom surfaces to determine the total heat transferred across the boundary in each case. These values are then added together to form the solution to case 1. In this way the relevant heat fluxes are related to the node temperatures. A similar approach was used for the temperature distribution in the bottom piece, but the boundary conditions were slightly different. For that case the top boundary is $T_6$ until the side element part, $T_5$ in the side element part, and an insulated boundary condition is applied to the bottom surface. The boundary conditions for the left and right side remain insulated due to symmetry.

A steady-state heat balance is performed at the solid-interface to relate the fluid temperature to the known values. The following relationship is obtained:

$$\frac{dT}{dz} = \frac{hs(T_{wall} - T)}{\rho c_p A_{hole} V} \qquad (14)$$

Where h represents the convection coefficient, s the perimeter of the channel, T is the fluid temperature at the given z position, and $T_{wall}$ the arithmetic average of the four channel side temperatures. The system of equations from the thermal network are solved to determine $T(z)$ and then from that all other temperatures of interest are derived. For detailed information on how to set up and solve a thermal resistance network please see a heat transfer textbook. To view the detailed formulation of a similar application, consult the recent work done by Valdevit et al.[10]

## VII.  Conclusions and Future Work

### A.  Conclusions
Initial attempts at developing a systematic method to determine an optimal layout for a heat sink have proven unsuccessful. Both framing the problem and determining a valid performance metric for ranking different designs have proven significantly more difficult than anticipated. The majority of this work has been done with a constant surface temperature boundary condition which has consistently led to designs with one large square channel located close to the hot surface being shown as the best solution. This result is in contrast to current designs and leads one to believe that the problem to be solved has not been adequately formulated.

The greatest challenge remaining is how to frame the problem so that appropriate optimization techniques can be applied. As the skin cooling of a hypersonic vehicle application has shown, this research does have practical applications and will continue to become more important in the near future. While this research has not resulted in the desired performance metric, it is hoped that the lessons learned from this study may be used by future researchers to develop the potential of heat sinks made from cellular materials.

### B.  Future Work
There are many parameters that one is able to consider for a heat sink and it is believed that improvements to current conventional designs may be obtained. This paper has shown the difficulty in using a fixed temperature boundary condition for the hot surface; however simulations using a constant heat flux boundary condition have not been examined. Further research should be done in this area to determine what results may be obtained. Similarly, the introductory thermal resistance network approach presented above should be completed and simulations run to determine whether the results offer improvements to similar thermal resistance networks.

There are several technologies which have great potential to improve current heat sinks. Cellular materials allow one to manufacture designs down to a very small scale. Coiled tubes hold great promise in being able to offer greater performance than

conventional straight tubes. Additional passive enhancements techniques, such as deliberately increasing the roughness of the tubes for greater fluid mixing could be considered. Active techniques could also be employed. Once a valid performance metric is established, the viability of more complex channel shapes such as triangles, rectangles, and ovals may be considered. Optimization techniques such as the Taguchi Method are expected to greatly reduce the number of simulations necessary for evaluating different designs.

Once the development of an optimal heat sink becomes more mature, one could move from focusing on this single component to integrating it into a full thermodynamic cycle for use in an application like skin cooling of a hypersonic vehicle. The feasibility of manufacturing several near optimal designs should also be investigated. If the construction of these designs proves viable, experimental testing to check the validity of the analytical model developed should be performed.

## References

[1] Incropera, F., and DeWitt, D., *Fundamentals of Heat and Mass Transfer,* 4th ed., Wiley, USA, 1996, pp. 618, 433, 436.

[2] Gibson, L. J., and Ashby, M. F., *Cellular Solids: Structure and properties*, 2nd ed., Cambridge University Press, United Kingdom, 1997, Chap. 1.

[3] Webb, R. L., and Kim, N. H., *Principles of Enhanced Heat Transfer,* 2nd ed., Taylor & Francis Group, NY, 2005, Chap. 1.

[4] Afimiwala, K.A., Mayne, R. W., and Shah, R.K., "Heat Exchanger Optimization," *Proceedings of the Sixth International Heat Transfer Conference*, Toronto, Canada, 1978, pp. 185-191.

[5] Acharya, N., Sen, M., and Chang, H. C., "Analysis of Heat Transfer Enhancements in Coiled-Tube Heat Exchangers," *International Journal of Heat and Mass Transfer,* Vol. 44, 2000, pp. 3189-3199.

[6] Palais, R. S., "Helix," *3D-XplorMath Space Curve Gallery,* 2004-2006, URL: http://rsp.math.brandeis.edu/3d-xplormath/SpaceCurves/helix/helix.html [cited 12 March 2007]

[7] Pluntze, S. C., And Eberhardt, D. S, *Application of Taguchi Techniques to the Evaluation of a CFD Solver,* 1998, URL:
http://www.aa.washington.edu/faculty/eberhardt/Taguchi.pdf [cited 12 March 2007]

[8] Faghri, A., *Heat Pipe Science and Technology*, Taylor & Francis Group, NY, 1995.

[9] NASA Dryden Flight Research Center, "Computational Fluid Dynamics (CFD) Image of Hyper-X research Vehicle at Mach 7 with engine operating," *X-43A Hyper-X Photo Collection*, Photo number ED97-43968-1, 1997, URL: http://www.dfrc.nasa.gov/Gallery/Photo/X-43A/HTML/ED97-43968-1.html [cited 12 March 2007].

[10] Valdevit, L., Vermaak, N., Hsu, K., Zok, F. W., and Evans, A. G., "Design of Actively Cooled Panels for Scramjets," *Proceedings of the 14th AIAA/AHI Space Planes and Hypersonic Systems and Technologies Conference,* AIAA, Washington, DC 2006-8069, 2006.